Interstellar C3 toward HD 210121

Evelyne Roueff, Paul Felenbok, John H. Black, Cecile Gry

A&A 384, 629–637 (2002)
DOI: 10.1051/0004-6361:20020067

Astronomy & Astrophysics

Interstellar C_3 toward HD 210121⋆

E. Roueff[1], P. Felenbok[2], J. H. Black[3,⋆⋆], and C. Gry[4]

[1] LUTH and FRE 2462 du CNRS, Observatoire de Paris-Meudon, 92195 Meudon, France
e-mail: Evelyne.Roueff@obspm.fr
[2] LESIA and FRE 2461 du CNRS, Observatoire de Paris-Meudon, 92195 Meudon, France
e-mail: Paul.Felenbok@obspm.fr
[3] Centre for Astrophysics and Space Science, Chalmers University of Technology, Onsala Space Observatory, 43992 Onsala, Sweden
e-mail: jblack@oso.chalmers.se
[4] ISO Data Center, ESA Research and Scientific Support Department, PO Box 50727, 28080 Madrid, Spain
e-mail: cgry@iso.vilspa.esa.es

Received 9 August 2001 / Accepted 7 January 2002

Abstract. We report the detection of the 405 nm band of interstellar C_3 in absorption toward HD 210121. The abundance of triatomic carbon is approximately 1/17 of that of diatomic carbon in the same diffuse molecular cloud. Rotational levels of C_3 up to $J = 14$ are seen in this cloud. The rotational excitation of C_3 in the interstellar medium may reflect a competition between inelastic collisions, formation and destruction of the molecule, and radiative pumping in the far-infrared. The abundance of C_3 is compared with chemical models. Attention is called to molecular properties that need to be better determined.

Key words. astrochemistry – molecular data – molecular processes – ISM: molecules

1. Introduction

In space as on Earth, carbon plays an important role in chemistry. Two distinguishing characteristics of interstellar chemistry are the presence of radicals and the prevalence of linear carbon-bearing molecules. The observed abundances of the largest linear molecules, such as $HC_{11}N$, challenge theories of interstellar chemistry. The simplest carbon-chain species, C_2 and C_3, can be observed in diffuse and translucent interstellar clouds where their abundances can be measured accurately. These clouds offer rigorous tests of models of interstellar chemistry. In particular, it is of interest to analyze the abundances of atomic carbon and of small carbon-bearing molecules in the same regions with the goal of improving our understanding of the processes that lead to the growth of larger molecules. The recent suggestion that C_7^- might be responsible for some of the diffuse interstellar bands (Tulej et al. 1998) focuses attention on the question raised by Douglas (1977) whether long chains might exist in detectable amounts even in the diffuse clouds.

Aside from the issues of molecular abundances, the simple forms of molecular carbon, C_2 and C_3, are both valuable spectroscopic diagnostic tools. Because these molecules have symmetrical structures in their ground states, they have no permanent dipole moments and thus lack allowed rotational spectra. Their rotational state populations would thus be well thermalized at the kinetic temperature were it not for the allowed radiative transitions in the visible and infrared that couple their excitation to the background radiation. This competition between radiative and collisional processes makes their rotational population distributions observable to high levels of excitation and sensitive to both density and temperature.

Triatomic carbon, C_3, was first tentatively identified in interstellar gas by Haffner & Meyer (1995). Previous searches had been unsuccessful (Snow et al. 1988; Clegg & Lambert 1982). The infrared spectrum of C_3 was measured in the circumstellar envelope of CW Leo (IRC +10216) by Hinkle et al. (1988), and in interstellar absorption toward Sgr B2 by Cernicharo et al. (2000). Giesen et al. (2001) discussed new laboratory data on the vibrational spectrum of C_3 in its low-frequency bending mode and re-visited an earlier tentative identification of the ν_2 R(2) line in absorption toward Sgr B2

Send offprint requests to: E. Roueff,
e-mail: Evelyne.Roueff@obspm.fr

⋆ Based on observations collected at the European Southern Observatory, Paranal, Chile [ESO VLT-UT2 No 65.I-0526(A)].

⋆⋆ Visiting Astronomer, LUTH, Observatoire de Paris-Meudon.

(Van Orden et al. 1995). The abundance and excitation of C_3 in diffuse clouds were measured convincingly by Maier et al. (2001) toward three stars. It is in such diffuse clouds where the chemistry and physics of non-polar carbon chain molecules can be studied in greatest detail, indeed Maier et al. (2001) detect C_3 in rotational states as high as $J = 30$, which lies 399.27 cm^{-1} (574 K) above the ground level. We present here new observations of C_3 in the well studied translucent molecular cloud toward HD 210121. Analysis of the rotational excitation shows that radiative pumping by the Galactic background radiation, mainly in the ν_2 vibrational transition, may play an important role in populating excited levels.

2. Observations and results

The observations were performed at the European Southern Observatory, Paranal, Chile, on the UV-Visual Echelle Spectrograph (UVES) fixed on a Nasmyth platform of the second VLT unit 8.2 m telescope KUYEN. UVES is a high-resolution cross-dispersed echelle spectrograph (Dekker et al. 2000), with separate blue and red arms that can be used simultaneously with a dichroic beam splitter or in a single arm mode. We chose the blue arm in the single arm mode and centered the wavelength domain at 437 nm, with a total spectral range of 120 nm. We used a $CuSO_4$ filter to reject red stray light and a slit aperture of 0.4 arcsec without image slicer. The detector is an EEV CCD with 2048×4096 pixels used in a window of 2048×3000 pixels. With low-gain, 1×1 binning, the readout noise was around 4 electrons rms. The present data on HD 210121 were obtained in two exposures of 1200 s each during the the night of 2000 July 1. The seeing was $0\farcs7$, so that the image size was only slightly larger than the entrance aperture. The spectral resolution is $R = \lambda/\Delta\lambda \approx 69\,000$, measured on a thorium line at 4019.13 Å. The signal/noise ratio in the reduced spectrum is $S/N \approx 500$ for the sum of the two exposures. The data have been reduced with the UVES pipeline provided by ESO (Ballester et al. 2000) where non-standard parameters are required to take advantage of the high signal to noise achieved in such observations. Bias and flat field files were used in the conventional way and wavelength calibration was done with a ThAr lamp.

The stellar spectrum in the range 400–408 nm was fitted with cubic splines to running averages over 14 pixels and this smooth representation of the continuum was divided into the reduced spectra to yield interstellar absorption spectra on a relative intensity scale with a flat continuum at $I_c = 1.0$. The resulting spectrum containing interstellar K I and C_3 lines around 405 nm is shown in Fig. 1.

A finding list of lines in the C_3 $\tilde{A}$–$\tilde{X}$ (000)–(000) band is presented in Table 1, together with measured results. The columns contain (1) the designation of the line, (2) its rest wavelength in air, (3) the observed wavelength where measurable, (4) the apparent Doppler velocity of the line, (5) the equivalent width W in mÅ, (6) the oscillator strength f, and (7) the derived column density in the lower state N_J. The two lines of interstellar K I are included for reference. The average Doppler velocity of the C_3 lines is -37.4 km s^{-1}, which is in excellent agreement with the velocities measured for the K I lines, -37.1 and -37.4 km s^{-1}. Equivalent widths are tabulated only when they are comparable to or greater than the fitted uncertainties. The Q(16) line, for example, is not clearly detected. The estimated uncertainties in W are mostly ± 0.15 mÅ or less, which is in harmony with what is expected from the resolution $R = 69\,000$ and average signal/noise ratio $S/N \approx 500$ in the spectrum: $\delta W = \lambda/(R \cdot S/N) = 0.12$ mÅ. The mean line width of the C_3 lines is $\Delta\lambda = 0.051$ Å, full-width at half-maximum of the profile, which is 15 per cent smaller than the nominal resolution. Thus the C_3 lines appear to be unresolved, so that the Doppler broadening parameter must be $b \leq 2.3$ km s^{-1}. Measured widths of CO emission lines in the same translucent molecular cloud suggest that $b \approx 1$ km s^{-1} is appropriate (Gredel et al. 1992). As long as $b \geq 0.15$ km s^{-1} the column densities in the lower states N_J can safely be derived from the weak line limit of equivalent width, $W = 8.853 \times 10^{-21} \lambda^2 N_J f$ Å, where the wavelength λ is in Å and N_J is in units of molecules cm^{-2}.

The rest wavelengths for C_3 have been adapted from Gausset et al. (1965). Becker et al. (1979) have derived an electronic oscillator strength $f_{\rm el} = 0.0246$ from experimental lifetime measurements of electronically excited C_3 ($^1\Pi_u$). The corresponding absorption oscillator strength of the $\tilde{A}(0,0,0)$–$\tilde{X}(0,0,0)$ band is $f = 0.0146$, based on the Franck-Condon factors of Jungen & Merer (1980). This is 10 per cent smaller than the oscillator strength chosen by Maier et al. (2001) who used the Franck-Condon factors calculated by Radić-Perić et al. (1977). It is important to note that all of the C_3 lines are weak, $W \lesssim 1$ mÅ, and that several are blended as indicated in the table. The tabulated uncertainties correspond to one standard deviation in the noise and exclude systematic effects associated with the determinations of the continuum level and zero level in the spectrum. Even so, the molecule is detected in rotational states as high as $J = 14$.

We also searched in the same reduced spectra for evidence of the 1^1T_u–1^1A_g 0_0^0 vibronic band of the fullerene C_{60} at an expected wavelength of 4024.0 ± 0.5 Å (Sassara et al. 2001). This wavelength falls in the blue wing of the stellar He I 2^3P–5^3D multiplet; therefore, it is not possible to place a useful limit on interstellar C_{60} from this transition without an accurate representation of the stellar line profile.

3. The abundance and excitation of C_3

In order to determine the total column density and abundance of C_3, it may be necessary to account for molecules in unobserved levels. Although a simple thermal description of the rotational excitation fits the present data rather well, other considerations show that the excitation is likely to be more complicated.

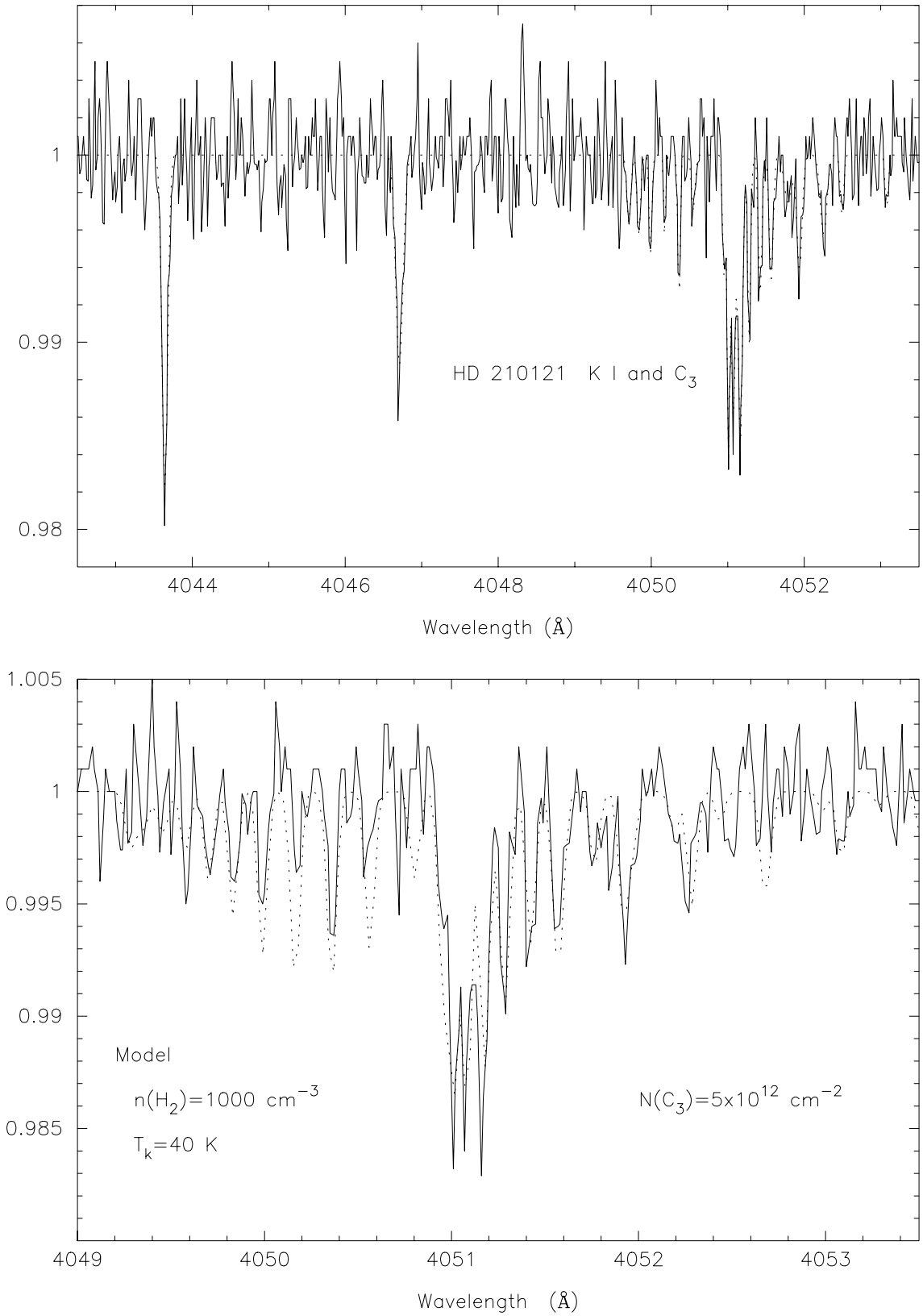

Fig. 1. Upper panel: the observed VLT/UVES spectrum of HD 210121 in the vicinity of the interstellar K I and C_3 lines. The vertical scale is relative intensity. Dotted curve shows the best fit of Gaussian profiles to all the measurable lines. Lower panel: dotted curve shows the computed spectrum based on the adopted excitation model, convolved to the resolution of the observed spectrum shown as a solid curve.

Table 1. Observations of C_3 toward HD 210121.

Line	λ(air)	λ(obs)	V	W	$10^3 f$	N_J
	Å	Å	$\mathrm{km\,s^{-1}}$	mÅ		10^{11} $\mathrm{cm^{-2}}$
K I	4044.143	4043.642 ± .0030	–37.1	1.67 ± .17	6.09	19 ± 2
K I	4047.213	4046.708 ± .0053	–37.4	1.36 ± .20	3.04	30 ± 5
R(24)	4049.769				3.87	
R(22)	4049.784				3.89	
R(26)	4049.784				3.86	
R(20)	4049.810				3.92	
R(28)	4049.810				3.84	
R(18)	4049.861				3.95	
R(30)	4049.861				3.83	
R(32)	4049.922				3.82	
R(16)	4049.963				3.98	
R(14)	4050.081	4049.583 ± .0079	–36.9	0.16 ± .10	4.03	2.8 ± 1.7
R(12)	4050.206	4049.707 ± .013	–36.9	0.24 ± .14	4.09	4.0 ± 2.4
R(10)	4050.337	4049.837 ± .0094	–37.0	0.25 ± .14	4.17	4.1 ± 2.2
R(8)	4050.495	4049.990 ± .0073	–37.4	0.25 ± .12	4.29	4.0 ± 1.9
R(6)	4050.670	4050.176 ± .0064	–36.5	0.15 ± .13	4.49	2.2 ± 1.9
R(4)	4050.866	4050.363 ± .0041	–37.2	0.32 ± .14	4.87	4.5 ± 2.0
R(2)	4051.069	4050.549 ± .012	–38.5	0.18 ± .14	5.84	2.1 ± 1.7
R(0)	4051.309			<0.28	14.6	<1.3
Q(2)	4051.461	4050.949 ± .0087	–37.9	0.28 ± .17	7.30	2.6 ± 1.6
Q(4)	4051.519	4051.006 ± .0037	–38.0	0.64 ± .20	7.30	6.0 ± 1.9
Q(6)	4051.590	4051.072 ± .0052	–38.3	0.97 ± .26	7.30	9.1 ± 2.5
Q(8)	4051.681	4051.165 ± .0040	–38.2b	1.10 ± .19b	7.30	9.7b
P(2)	4051.741	4051.165 ± .0040	–42.5b	1.10 ± .19b	1.46	3.1b
Q(10)	4051.793	4051.280 ± .0039	–38.0	0.50 ± .12	7.30	4.7 ± 1.2
Q(12)	4051.929	4051.423 ± .0056	–37.4	0.45 ± .13	7.30	4.2 ± 1.2
P(4)	4052.062	4051.568 ± .0066b	–36.5b	0.44 ± .15b	2.43	4.8b
Q(14)	4052.089	4051.568 ± .0066b	–38.5b	0.44 ± .15b	7.30	2.6b
Q(16)	4052.271	4051.790 ± .066	–35.6	0.33 ± .43	7.30	≤4.1
P(6)	4052.424	4051.937 ± .0098	–36.0	0.52 ± .27	2.81	12.6 ± 6.7
Q(18)	4052.473				7.30	
Q(20)	4052.698				7.30	
P(8)	4052.792	4052.254 ± .013	–39.8	0.47 ± .19	3.00	10.8 ± 4.3
Q(22)	4052.940				7.30	
P(10)	4053.180				3.13	
Q(24)	4053.208				7.30	
Q(26)	4053.490				7.30	
P(12)	4053.591				3.21	
Q(28)	4053.794				7.30	
P(14)	4054.020				3.27	
Q(30)	4054.112				7.30	
Q(32)	4054.450				7.30	
P(16)	4054.458				3.32	
P(18)	4054.908				3.35	
P(20)	4055.373				3.38	
P(22)	4055.877				3.40	
P(24)	4056.410				3.42	
P(26)	4056.961				3.44	
P(28)	4057.531				3.45	
P(30)	4058.121				3.47	
P(32)	4058.729				3.48	

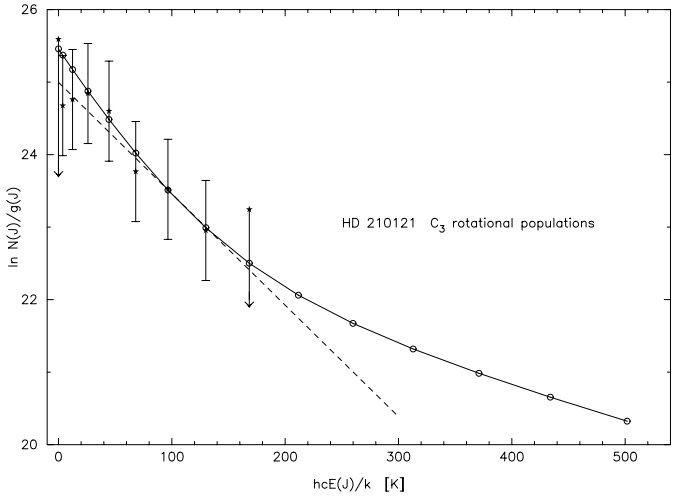

Fig. 2. Population distributions of C_3: the solid stars with error bars or limits are the observed column densities, the solid curve connecting open circles indicates the population distribution of the full excitation model, and the dashed curve shows a simple thermal Boltzmann population at 65 K.

3.1. Thermal excitation

The observations yield only an upper limit on the column density in $J = 0$. The sum of column densities in detected states is

$$\sum_{J=2}^{14} = 3.5 \times 10^{12} \quad \mathrm{cm}^{-2},$$

and the observed distribution of populations is shown as error bars in Fig. 2. In such a graph of $\ln N_J/g_J$ versus the energy E_J of state J, a constant value of rotational excitation temperature $T_{\rm rot}$ would correspond to a straight line with a slope inversely proportional to the value of $T_{\rm rot}$. The dashed line in Fig. 2 represents a total column density of $N(\mathrm{C_3}) = 3.79\times10^{12}$ cm^{-2} at $T_{\rm rot} = 65$ K and is the best fitting straight line. This apparent population distribution is very similar to those observed in levels $J \leq 14$ by Maier et al. (2001) in diffuse molecular clouds. The measurements of Maier et al. (2001) also show a second distribution of higher excitation temperature $T_{\rm rot} \sim 200-300$ K in states $J > 14$.

3.2. The need for a detailed model of C_3 excitation

Because C_3 is a symmetrical, linear molecule in its ground electronic state, radiative transitions between rotational levels are dipole-forbidden and occur only as weak, electric quadrupole transitions. The quadrupole moment of C_3 is not known; therefore, we adopt the electric quadrupole moment of C_2, $Q = 2.26$ AU (van Dishoeck & Black 1982). The spontaneous transition probabilities for pure rotational transitions lie in the range $A(J + 2, J) = 1.3 \times 10^{-20}$ s^{-1} at $J = 0$ to 9.0×10^{-13} s^{-1} at $J = 48$. Rotational level populations would thus easily be thermalized at interstellar densities if there were no other interactions of C_3 molecules with their environment. C_3 has allowed vibration-rotation transitions in the ν_2 bending mode (fundamental frequency 63 cm^{-1}) and in the ν_3 asymmetric stretching mode (fundamental frequency 2040 cm^{-1}), which cause its excitation to be coupled to the background radiation at infrared and far-infrared wavelengths. C_3 also absorbs visible starlight in the $\tilde{\mathrm{A}}$–$\tilde{\mathrm{X}}$ electronic system. The populations of excited rotational and vibrational states will thus be determined by a combination of collisional and radiative processes, which should be able to achieve a steady state within time-scales of the order of 1 year or less. The adopted model of the average background radiation (Black 1994) combines the 2.7 K cosmic background, the far-IR and submillimeter background derived from COBE measurements (Wright et al. 1991), and the infrared, visible, and UV radiation of stars and dust (Mathis et al. 1983). The collision rates are assumed to be proportional to the radiative line strengths and are scaled to a constant downward rate coefficient $q_{u\ell} = 2.0 \times 10^{-11}$ cm^3 s^{-1}. The mean Galactic background radiation induces absorption in C_3 at typical rates of 2×10^{-20} s^{-1}, 5×10^{-8} s^{-1}, 1.3×10^{-10} s^{-1}, and 6×10^{-10} s^{-1} in the quadrupole $J = 2 \leftarrow 0$ pure rotational transition, the ν_2 vibrational band, the ν_3 vibrational band, and the $\tilde{\mathrm{A}}(0, 0, 0)$–$\tilde{\mathrm{X}}(0, 0, 0)$ vibronic band, respectively. It is evident that radiative processes will compete effectively with collisions in controlling the rotational excitation at interstellar densities $n \lesssim 10^3$ cm^{-3}. Inelastic collisions change J by ±2 in this simple model. Absorption in a dipole-allowed R-branch transition followed by spontaneous emission in a P-branch transition increases J by 2 quanta, while P-branch absorption followed by R-branch emission decreases J by 2. The important absorptions occur in quite different parts of the spectrum where the radiation brightness temperature can have values near 7 K (far-IR), 100 K (near-IR), and 1000 K (visible).

Very little is known about the ultraviolet spectrum of C_3. Chang & Graham (1982) observed ultraviolet absorption of carbon trapped in an argon matrix at 8 K and attributed it to the $1^1\Sigma_u^+$–$\tilde{\mathrm{X}}^1\Sigma_g^+$ band system of C_3 originating near 189 nm wavelength. Forney et al. (1996) discussed properties of larger linear carbon molecules and estimated by extrapolation that a strong $^1\Sigma_u^+$–$\tilde{\mathrm{X}}^1\Sigma_g^+$ band might appear in C_3 around 170 nm wavelength, which is in harmony with the computation of Kolbuszewski (1995) and is close to the expected dissociation threshold. The absorption rate in an ultraviolet transition of oscillator strength $f = 1$ at 170 nm would be 3.0×10^{-9} s^{-1} for our adopted model of the background radiation. It is likely that such transitions are strongly predissociated and thus contribute little to the fluorescent excitation of C_3. Even with 100% fluorescent efficiency and no attenuation of ultraviolet radiation by dust, the ultraviolet pumping rate would be less than 1/10 that in the ν_2 vibrational band; therefore, neglect of ultraviolet pumping is unlikely to affect our model of the excitation. The effect of dissociating ultraviolet radiation is incorporated into the excitation model as part of the destruction rate.

Multi-level excitation calculations for interstellar molecules often overlook the effect of formation and destruction processes on the rotational populations. In the present case of C_3 in diffuse clouds, the rate of photodissociation by ultraviolet starlight alone could be higher than 10^{-9} s^{-1} (van Dishoeck 1988). This would imply that a C_3 molecule will suffer of the order of 10 excitations during its lifetime: even so, the highest rotational levels may owe their excitation to the formation process itself, with some re-arrangement by the other processes. In this way, the apparent excitation temperatures of the high-J levels may be more closely related to the molecular dynamics of the main chemical source reaction than to the kinetic temperature or any of the radiation temperatures. This hypothesis is confirmed by detailed calculations of the multi-level excitation of a 154-state C_3 molecule.

Details of the adopted molecular data and the excitation model will be discussed in a separate publication. Briefly, all levels $J \leq 50$ in the $\tilde{X}$ (0, 0, 0), (0, 1, 0), (0, 0, 1) and $\tilde{A}$ (0, 0, 0) vibronic states are included. All electric quadrupole transitions within the ground vibronic state and all allowed dipole transitions between states are included in the radiative excitation. The levels of $\tilde{X}$ (0, 0, 0) and (0, 1, 0) are assumed to be collisionally coupled according to the simple description of inelastic collision rates with H_2 as outlined above. The destruction rates are assumed to be identical for all levels and are taken as an input parameter. The initial distribution of populations in newly formed C_3 molecules is parametrized as a Boltzmann distribution at a formation temperature T_f. With the assumption of steady state, the total formation rate is fixed by the specified values of the fractional abundance relative to H_2, the H_2 density, and the C_3 destruction rate. The resulting system of rate equations is solved for 154 states of C_3 and the computed column densities and line intensities can then be compared with observation.

The present data on HD 210121 do not determine the C_3 abundances in states $J > 14$ well enough to constrain the full excitation model. Thus we appeal to independent estimates of density and temperature in order to illustrate the predicted effects. The various observations of the translucent cloud toward HD 210121 summarized by Gredel et al. (1992) suggest a density in the range $n(H_2) = 250$ to 2500 cm^{-3} and a kinetic temperature $T \geq 20$ K. The column density of H_2 towards HD 210121 has been obtained by Rachford et al. (2002) from FUSE observations and $N(H_2) = (5.6 \pm 1.5) \times 10^{20}$ cm^{-2}. This is consistent with the previous indirect estimate, $N(H_2) = (8 \pm 2) \times 10^{20}$ cm^{-2}, of Gredel et al. (1992).

A full excitation model computed with $n(H_2) = 1000$ cm^{-3}, $T = 40$ K, a destruction rate of 3×10^{-9} s^{-1}, and a formation temperature $T_f = 300$ K has been adopted for comparison with the observations. The computed interstellar absorption spectrum based on this model is shown superimposed on the observed spectrum in the bottom panel of Fig. 1. The computed column densities are displayed on the excitation diagram in Fig. 2 as open circles connected by a solid curve for comparison with the observed column densities and the simple thermal model. The total column density $N(C_3) = 5 \times 10^{12}$ cm^{-2} corresponds to a fractional abundance $C_3/H_2 = 8.9 \times 10^{-9}$. This can be taken as an upper bound on the total amount of C_3 including unobserved levels. The formation temperature used here also yields a good representation of the high-temperature component of C_3 seen toward ζ Oph by Maier et al. (2001).

The detailed excitation model determines the populations in all excited levels of the molecule and thus provides predictions about its observability in other wavebands. The strongest transition in the predicted ν_2 vibrational spectrum will be the (0, 1, 0)–(0, 0, 0) Q(6) line at 157.26 μm wavelength: in the adopted model, its excitation temperature is 7.31 K and its line-center optical depth $\tau = 0.0041$ for an assumed line broadening of $b = 1$ km s^{-1}. The excitation temperature is slightly higher than the radiation brightness temperature of the background radiation; therefore, the line might appear weakly in emission from such a cloud. In practice, far-IR lines from such thin clouds are probably undetectably weak.

In summary, a simple thermal description of the excitation of C_3 yields a total column density 3.8×10^{12} cm^{-2} and an estimated fractional abundance of 6.75×10^{-9} relative to H_2. A detailed model of the excitation suggests that the total column density could be as high as 5×10^{12} cm^{-2}, but at a kinetic temperature, $T \leq 40$ K, that is smaller than the rotational excitation temperature implied by the simple thermal model, $T_{rot} = 65$ K. Although the data presented here do not demand the inclusion of radiative and chemical processes in the description of the rotational excitation of C_3, it is likely that such processes are important.

3.3. Comparison with C_3 in diffuse clouds

The excitation model described in the preceding section has been applied to the observations of three diffuse molecular clouds published by Maier et al. (2001). The tabulated equivalent widths have been converted to column densities in the unsaturated limit with use of the same oscillator strength applied to our data. An average column density $N(J'')$ for each lower level J'' has been calculated from the unblended lines only. The excitation models have been computed with different values of the parameters until the root-mean-square difference in $\ln N(J'')/(2J''+1)$ between observation and model is minimized. The total column density $N(C_3)$ of C_3 is taken to be one of the parameters in order to allow for unobserved levels. The total column density of H_2 is fixed by previously published observations, and the fractional abundance $x(C_3)$ is defined with reference to H_2. In all cases, the same background radiation field has been adopted (see Sect. 3.2). The other disposable parameters are thus the density of collision partners, n_{coll}; the kinetic temperature, T_k;

Table 2. Comparison of model analyses of C_3.

Star	$N(C_3)$	$N(H_2)$	$x(C_3)$	n_{coll}	T_k	D	T_f
	10^{12} cm^{-2}	10^{20} cm^{-2}	10^{-9}	cm^{-3}	K	10^{-9} s^{-1}	K
HD 210121	5	8	6.25	1000	40	3	300
ζ Oph	2.0	4.2	4.8	400	30	3.3	300
ζ Per	1.5	4.8	3.1	350	50	2.5	275
20 Aql	2.9	6.6	4.4	425	30	2.5	350

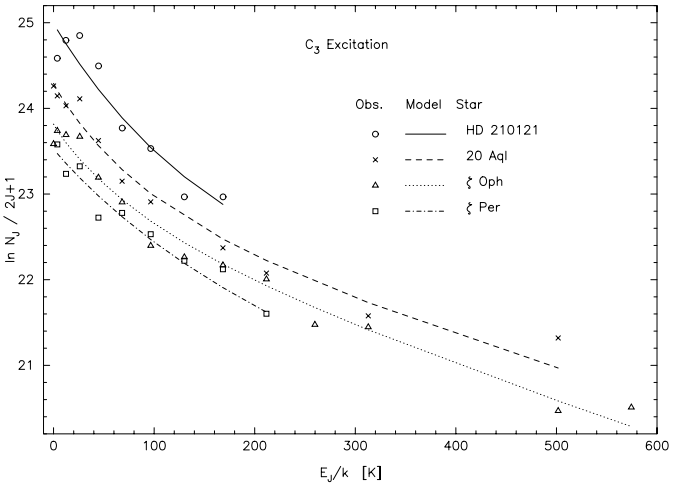

Fig. 3. Observed and calculated column densities N_J of levels J are compared for HD 210121 and the three stars observed by Maier et al. (2001). The horizontal axis is the excitation energy of level J in terms of temperature.

the destruction rate of C_3, D; and the formation temperature, T_f. The results for the best fitting models are summarized in Table 2.

Although one might presume that the density of collision partners is approximately equal to the density of H_2 in the molecular zones of these diffuse and translucent clouds, the derived density is called n_{coll} to remind the reader that it is uncertain because the inelastic collision rates are unknown. The adopted downward collision rate coefficient is $q_0 = 2 \times 10^{-11}$ cm^3 s^{-1}, independent of temperature. This corresponds to an inelastic cross section $\sigma_0 = 2.7 \times 10^{-16}$ cm^2 for $H_2 + C_3$ collisions at $T_k = 50$ K. This scaling of the collision rates yields derived densities that are consistent with other estimates for the same clouds. Even though the derived densities are uncertain, their relative values are meaningful: the excitation of C_3 suggests that the absorbing cloud toward HD 210121 is more than twice as dense as the diffuse clouds toward ζ Oph, ζ Per, and 20 Aql. The model analysis yields similar values in all four clouds of the other parameters. Figure 3 displays the comparison between observations and the models described above.

4. The chemistry of C_3

The abundance of C_3 in diffuse clouds was predicted first by Mitchell et al. (1978) in the context of ion-molecule reactions. In a chain of exothermic reactions involving the insertion of carbon ions with CH, C_2H until the formation of C_3H^+, C_3 is formed from the recombination of the C_3H^+ ion since the reaction between C_3H^+ and molecular hydrogen is slightly endothermic and the radiative association reaction rate coefficient is low. The main destruction mechanism of C_3 in diffuse clouds is photodissociation although the corresponding cross sections are not accurately known. Neutral-neutral reactions involving atomic carbon have been found to be more efficient than previously expected (Chastaing et al. 1999; Haider & Husain 1993) even at low temperatures, and Bergeat & Loison (2001) have shown that the channel toward C_3, involving an intersystem crossing mechanism makes a non-negligible contribution to the $C + C_2H_2$ reaction. We have used our model of a photon dominated region (Le Bourlot et al. 1993), recently updated by a more realistic model of the photoelectric effects on grains (Bakes & Tielens 1994). The atomic and molecular abundances are calculated as a function of the visual extinction of a translucent cloud of plane parallel geometry, illuminated on one side by the interstellar ultraviolet radiation field. The atomic to molecular transition is explicitly obtained from the radiative transfer of the ultraviolet interstellar field in the dissociating lines of H_2 and CO and in the continuous absorption by dust as given by the grain model 2 referred to in van Dishoeck (1988). The thermal balance is obtained from the equilibrium between the different cooling and heating mechanisms. The structure of the translucent cloud towards HD 210121 has been previously studied by Gredel et al. (1992) through millimeter-wave observations of CO, complemented with further measurements of CN and optical observations of C_2, CH, and CN (Gredel et al. 1991). Polyatomic species were sought but not found and the observed abundances and their upper limits were then interpreted with densities 500–5000 cm^{-3} and a low incident radiation field. We have used the chemical network provided by UMIST (Millar et al. 1997) and the density and temperature conditions of the model 2 of Gredel et al. (1992). The line of sight toward HD 210121 is known to produce anomalies in its extinction curve as recently discussed by Barbaro et al. (2001) and Larson et al. (2000), who note a relative excess of small grains compared with the average diffuse interstellar medium. The resulting ratio of total to selective extinction has a small value, $R_V = 2.1$, which implies $A_V < 1$ mag for the color index $E(B-V) = 0.4$. We explicitly introduce into the model the extinction curve of the HD 210121 cloud with the UV extinction curve fit

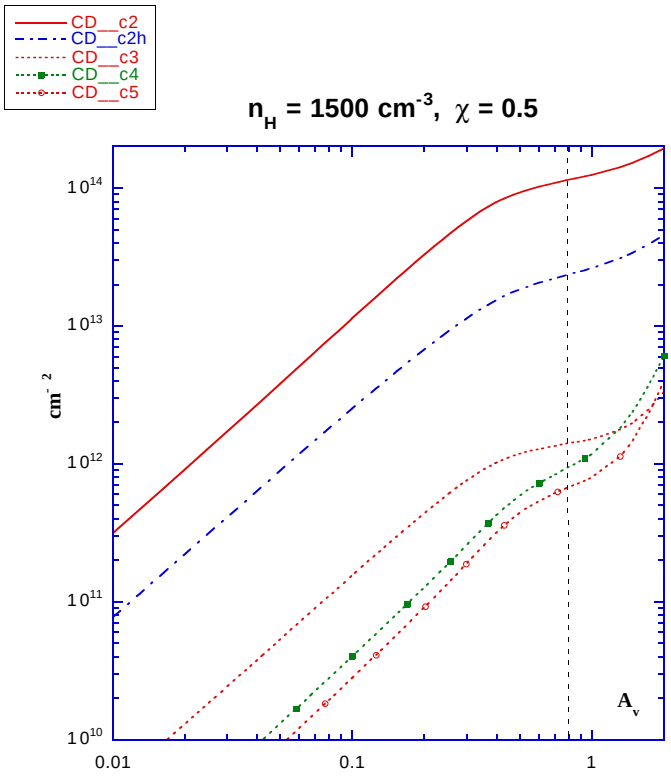

Fig. 4. Steady state solutions for the translucent cloud model of HD 210121. The column densities are displayed as functions of the visual extinction. The vertical dashed line corresponds to the visual extinction of HD 210121.

parameters of Welty & Fowler (1992) and a range of grain radii between 0.02 and 0.3 μm with a power law size distribution of 3.5 in the exponent. The small grains have a larger surface area per volume for hydrogen formation and contribute to the high molecular column densities towards this star. Figure 3 displays the calculated values of the column density of small carbon species, C_2, C_2H, C_3, C_4 and C_5 as functions of the visual extinction A_V.

5. Conclusions

We have presented an observation of C_3 molecules in the translucent molecular cloud toward HD 210121. Excited rotational levels are observed to $J \leq 14$. The observed column density of C_3 is 3.8×10^{12} cm^{-2}, approximately 1/17 times that of C_2 in the same cloud. Although the observed rotational excitation is consistent with a thermal Boltzmann distribution at $T_{\rm rot} = 65$ K, additional radiative and chemical processes may be important in the excitation. If so, then the kinetic temperature may be lower than $T_{\rm rot}$ and the total column density including highly excited states could be as high as 5×10^{12} cm^{-2}. A chemical model has been computed, which incorporates the peculiarities of the dust in this translucent cloud. The model explains the observed abundance of C_2 and reproduces the C_3 within a factor of 2.7, rather good agreement considering the uncertainties in rates of crucial processes. The chemical model suggests that larger carbon-chain molecules like C_4 may be detectable in such clouds.

Several molecular processes involving C_3 deserve further attention. If the rotational population distributions are to be useful as physical diagnostics, then it will be essential to have a better understanding of the cross sections of rotationally inelastic collisions of C_3 with H_2. These are completely unknown at present. In diffuse and translucent clouds, the abundance of C_3 may be limited by photodissociation by UV starlight: a detailed study of the photodissociation processes would be valuable. There is some evidence of an ultraviolet band system of C_3 in the wavelength range 170–189 nm, but it has not been characterized spectroscopically in the gas phase. Finally, a reaction of C_3 with H_2 to form C_3H, although perhaps not likely at low temperature, is nevertheless exoergic. If effective at interstellar temperatures, it could be both a sink of C_3 and a source of C_3H.

Note added in proofs: Since our paper has been submitted, Maier et al. (2002) have reported observational upper limits on C_4 and C_5 column densities towards ζ Ophiuchii of respectively 4×10^{12}–10^{13} and 2×10^{11} cm^{-2}. These values are in agreement with our chemical predictions for a cloud of visual extinction of about 1 mag or less.

Acknowledgements. Research in atomic and molecular astrophysics at Chalmers University of Technology is supported by the Swedish Natural Sciences Research Council and the Swedish National Space Board. ER is grateful to Drs Rachford and Snow who provided FUSE results on molecular Hydrogen towards HD 210121 before publication

References

Bakes, E. L. O., & Tielens, A. G. G. M. 1994, ApJ, 427, 822
Ballester, P., Modigliani, A., Boitquin, O., et al. 2000, The Messenger, Nr. 101, 31
Barbaro, G., Mazzei, P., Morbidelli, L., Patriarchi, P., & Perinotto, M. 2001, A&A, 365, 157
Becker, K. H., Tatarcyk, T., & Radić-Perić, J. 1979, Chem. Phys. Lett., 60, 502
Bergeat, A., & Loison, J. C. 2001, Phys. Chem. Chem. Phys., 3, 2038
Black, J. H. 1994, in The First Symposium on the Infrared Cirrus and Diffuse Interstellar Clouds, ed. R. M. Cutri, & W. B. Latter, ASP Conf. Ser., 58, 355
Black, J. H., & Dalgarno, A. 1973, ApJ, 184, L101
Cernicharo, J., Goicoechea, J. R., & Caux, E. 2000, ApJ, 534, L199
Chang, K. W., & Graham, W. R. M. 1982, J. Chem. Phys., 77, 4300
Chastaing, D., James, P. L., Sims, I. R., & Smith, I. W. M. 1999, Phys. Chem. Chem. Phys., 1, 2247
Clegg, R. E. S., & Lambert, D. L. 1982, MNRAS, 201, 723
Dekker, H., D'Odorico, S., Kaufer, A., Delabre, B., & Kotzlowski, H. 2000, Proc. Conf. SPIE, 4008-61
Douglas, A. E. 1977, Nature, 269, 130
Forney, D., Freivogel, P., Grutter, M., & Maier, J. P. 1996, J. Chem. Phys., 103, 4954
Gausset, L., Herzberg, G., Lagerquist, A., & Rosen, B. 1965, ApJ, 142, 45

Giesen, T. F., Van Orden, A. O., Cruzan, J. D., et al. 2001, ApJ, 551, L181; erratum, 2001, ApJ, 555, L77
Gredel, R., van Dishoeck, E. F., & Black, J. H. 1991, A&A, 251, 625
Gredel, R., van Dishoeck, E. F., Vries, C. P. de, & Black, J. H. 1992, A&A, 257, 245
Haffner, L., Matthew, & Meyer, D. M. 1995, ApJ, 453, 450
Haider, N., & Husain, D. 1993, J. Chem. Soc. Faraday Trans., 89, 7
Hinkle, K. W., Keady, J. J., & Bernath, P. F. 1988, Science, 241, 1319
Jungen, Ch., & Merer, A. J. 1980, Mol. Phys. 40, 95
Kolbuszewski, M. 1995, J. Chem. Phys., 102, 3679
Larson, K. A., Wolff, M. J., Roberge, W. G., Whittet, D. C. B., & He, L. 2000, ApJ, 532, 1021
Le Bourlot, J., Pineau des Forêts, G., Roueff, E., & Flower, D. 1993, A&A, 267, 233
Maier, J. P., Lakin, N. M., Walker, G. A. H., & Bohlender, D. A. 2001, ApJ, 553, 267
Maier, J. P., Walker, G. A. H., & Bohlender, D. A. 2002, ApJ, 566, 332
Mathis, J. S., Mezger, P. G., & Panagia, N. 1983, A&A, 128, 212
Millar, T. J., Farquhar, P. R. A., & Willacy, K. 1997, A&AS, 121, 139
Mitchell, G. F., Ginsburg, J. L., & Kuntz, P. J. 1978, ApJS, 231, 456
Rachford, B., Snow, T. et al. 2002, ApJ, submitted
Radić-Perić, J., Roemelt, J., Peyerimhoff, S. D., & Buenker, R. J. 1977, Chem. Phys. Lett., 50, 344
Rousselot, P., Arpigny, C., Rauer, H., et al. 2001, A&A, 368, 689
Sassara, A., Zerza, G., Chergui, M., & Leach, S. 2001, ApJS, 135, 263
Snow, T. P., Seab, C. G., & Joseph, C. L. 1988, ApJ, 335, 185
Spitzer, L., Jr., & Zweibel, E. G. 1974, ApJ, 191, L127
Tulej, M., Kirkwood, D. A., Pachkov, M., & Maier, J. P. 1998, ApJ, 506, L69
van Dishoeck, E. F. 1988, in Rate coefficients in Astrochemistry, ed. T. J. Millar, & D. A. Williams (Dordrecht: Kluwer), 49
van Dishoeck, E. F., & Black, J. H. 1982, ApJ, 258, 533
Van Orden, A., Cruzan, J. D., Provencal, R. A., et al. 1995, in Airborne Astronomy Symp. on the Galactic Ecosystem, ed. M. R. Haas, J. A. Davidson, & E. F. Erickson, ASP Conf. Ser., 73, 67
Welty, D. E., & Fowler, J. R. 1992, ApJ, 393, 193
Wright, E. L., Mather, J. C., Bennett, C. L., et al. 1991, ApJ, 381, 200